Effect of islands and rotation on neoclassical tungsten impurity transport

A. Bergmann

Max-Planck-Institut für Plasmaphysik, 85748 Garching, Germany

Recently, results on the tungsten impurity transport in JET have been reported [1], where it was found that NTMs can cause higher W densities in the center due to the suppression of the turbulent outward transport in the island. Here results on the effect of islands and fast toroidal rotation on the neoclassical transport of W45+ ions in a hot Tokamak plasma are reported. The neoclassical transport is caused by the collisions between main ions and impurities. Guiding centre particle simulations with the code HAGIS [2] were performed. The simulations are done in two steps, assuming the trace limit for the W ions. First, the density and temperature profiles and the parallel velocity of the main ions (D) are obtained from a simulation with D-D collisions but without D-W collisions. Then a simulation for W ions with W-D collisions is made. An equilibrium with concentric circular surfaces is used, so that the helical flux surfaces of the islands can be calculated analytically [3] for constructing a grid aligned to the helical flux surfaces. HAGIS is a δf code, the guiding center distribution function is split, $f_0 + \delta f$, where f_0 is a Maxwellian and δf is represented by marker particles [2]. In the simulations for tungsten f_0 is centered around the D parallel velocity. In case of strong toroidal rotation f_0 includes a poloidal variation taking into account that the centrifugal force causes a strong density variation if the Mach number is high. The evolution of the weights for δf is calculated from the full change of f_0 along the orbits and the contribution of the collisions [3]. The simulations are made in the lab frame, but for W the effect of the collisions is calculated in a frame moving with the D parallel velocity, $u_{i\|}$, and the D distribution function is approximated by a Maxwellian around $u_{i\|}$. In steady state the flux-friction relation holds for the flux surface averaged radial particle flux and the flux surface averaged parallel friction force divided by ZeB_p (B_p: poloidal magnetic field),

$$\Gamma_r = \left\langle \int (v_d \cdot \nabla r) f \, d^3v \right\rangle = -\left\langle \int \frac{v_\|}{\omega_{cp}} C(f) \, d^3v \right\rangle = -\left\langle \frac{R_\|}{ZeB_p} \right\rangle \tag{1}$$

In the simulation the radial W flux density is thus calculated in two ways: by summing up the radial component of the drift velocity and by summing up the collisional changes of the parallel momentum. The evolution of the radial W flux density in the transient phase of a simulation without radial electric field is shown in Fig. 1(a): while the flux determined from the collisional momentum change starts from zero and slowly approaches the final value, the sum of radial guiding centre motions first shows oscillations depending on the initial conditions. The term in

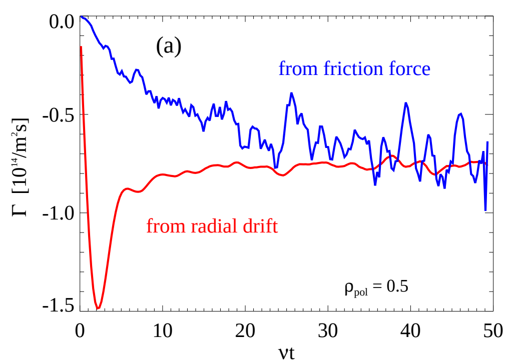

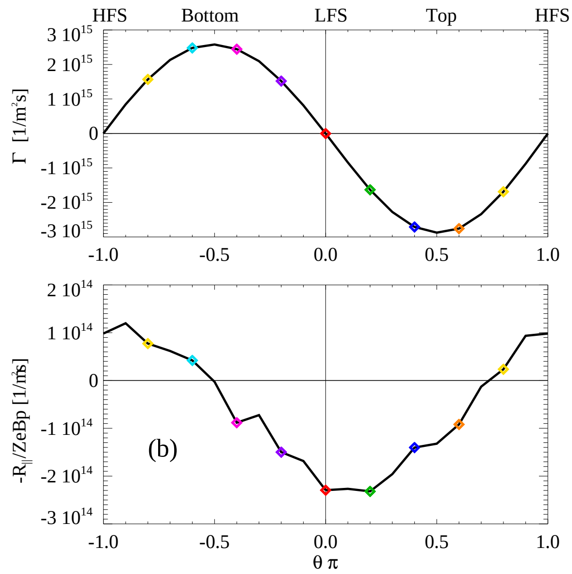

Fig. 1: (a)The time evolution of the surface averaged radial W flux calculated from the radial guiding centre drifts (red) or the parallel friction force (blue), (b) the poloidal variation of the local guiding centre flux (top) and of the local flux derived from the parallel friction (bottom) in steady state. Poloidal angle $\theta = 0$ at the outer midplane, $\theta = \pm\pi$ at the inner midplane. $\rho_{\rm pol} = 0.5$

the left most brackets in Eq. (1) is the local radial guiding centre flux (shown in Fig. 1(b)), which, in absence of strong poloidal electric fields, is given by the magnetic drift. With $p_{\|} = p_{\perp} = p$:

$$\int (v_d \cdot \nabla r)\, f\, d^3v = \frac{B \times \nabla B \cdot \nabla r}{ZeB^3} \int \left(\frac{m}{2} v_\perp^2 + m v_\|^2\right) f\, d^3v \approx -\frac{2p\,(1+M^2)}{ZeB_0 R_0} \sin\theta \qquad (2)$$

where $M^2 = m u_\|^2/2T$. This flux does not only contain the collisional transport but also the radial orbit motion. Therefore often the expression in the second or third bracket in Eq. (1) is taken as the local radial flux, it is also shown in Fig. 1(b). While the friction is strong near the midplane, the actual radial flux of guiding centres vanishes at the midplane. This is important for the case with high impurity Mach number, see below. Simulations with imposed (3/2)-islands of various sizes were made. The islands are stationary, in the cases with radial electric field they rotate with the plasma, $\omega/n = E_r/RB_p$ (taken at the resonant surface). In Fig. 2(a)

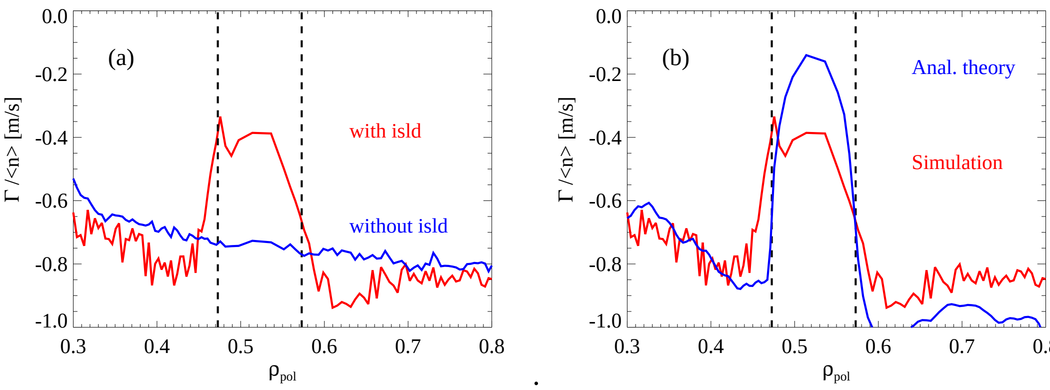

Fig. 2: The W flux is reduced in the island due to the flattening of the main ion density profile: (a) $\langle \Gamma_{Wr} \rangle / \langle n_W \rangle$ with and without island, (b) flux compared to analytic theory [4,5].

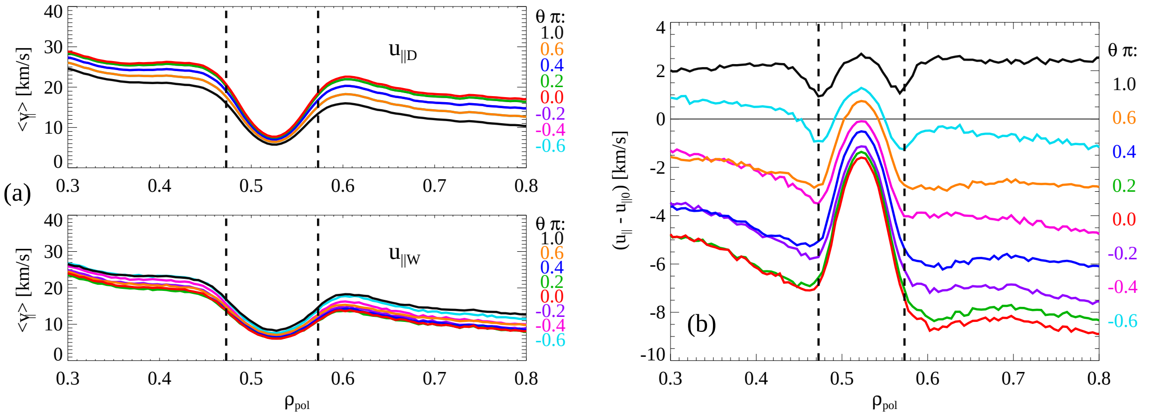

Fig. 3: The parallel velocities (left) of main ions (top) and impurities (bottom) and their difference (right) and thus the friction force are strongly reduced in the island. Colours denote poloidal angle.

results for the W flux with and without island are depicted. The transport is directed inwards, but it is reduced in the island due to the flattening of the main ion profiles. Fig. 2(b) shows a comparison with the analytic theory [4,5] (for flat temperature and small poloidal density variation), $\langle\Gamma_{Wr}\rangle/\langle n_W\rangle = -2q^2 Z(\nu_{ii}/\omega_{ci})(\rho_i/L_{ni})v_{T_i}$, where L_{ni} is gradient length and the index i refers to the main ions. The parallel velocities of main ions and impurities and their difference are strongly decreased in the island (Fig. 3), and consequently the friction force is also reduced. In presence of a strong radial electric field the same effect of the island on the flux is found (Fig. 4(a)). The transport is increased by the rotation by a factor ε^{-1} instead of ε^{-2} as given in [4,5]

$$\frac{\langle\Gamma_{Wr}\rangle}{\langle n_W\rangle} = -\frac{Zq^2}{\varepsilon^2}\frac{\nu_{ii}}{\omega_{ci}}\frac{\rho_i}{L_n}v_{T_i}\left(\left(\left\langle\frac{n_W}{B^2}\right\rangle - \left\langle B^2/n_W\right\rangle^{-1}\right)\frac{\langle B^2\rangle}{\langle n_W\rangle}\right) \tag{3}$$

Here, the tungsten Mach number is between 3 and 4, and the density of tungsten ions is localised at the low field side such that the bracket in Eq. (3) is of order unity. In conclusion, the usual neoclassical theory seems to be applicable to the island case (except for very small islands).

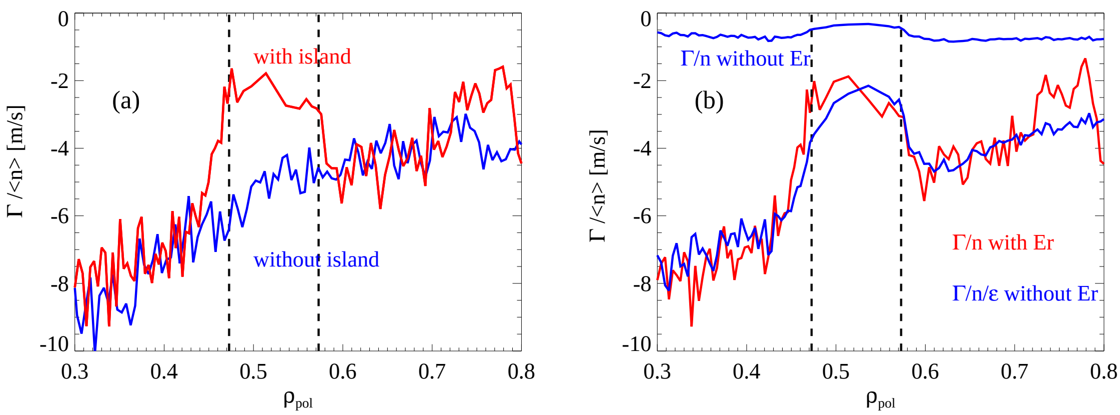

Fig. 4: Effect of island in the case of strong toroidal rotation. (a) $\langle\Gamma_{Wr}\rangle/\langle n_W\rangle$ with and without island, (b) $\langle\Gamma_{Wr}\rangle/\langle n_W\rangle$ compared to value for $E_r = 0$ as it is and divided by ε. The flux is enhanced by ε^{-1} at high Mach number.

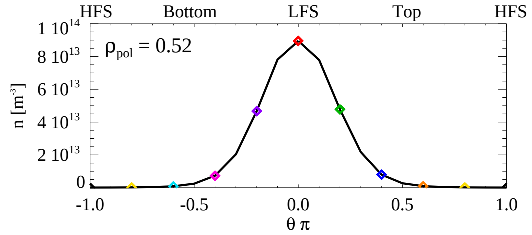

Fig. 5: The poloidal variation of the W45+ density in simulation with high Mach number (3–4) flow. $\rho_{\mathrm{pol}} = 0.52, < n >= 2.3 \cdot 10^{13}$

Strong toroidal rotation increases the local radial particle flux everywhere (except at the midplane). If the density is poloidally localised and shifted away from the midplane, the surface averaged radial flux increases strongly. This is demonstrated in Fig. 6 with results from the

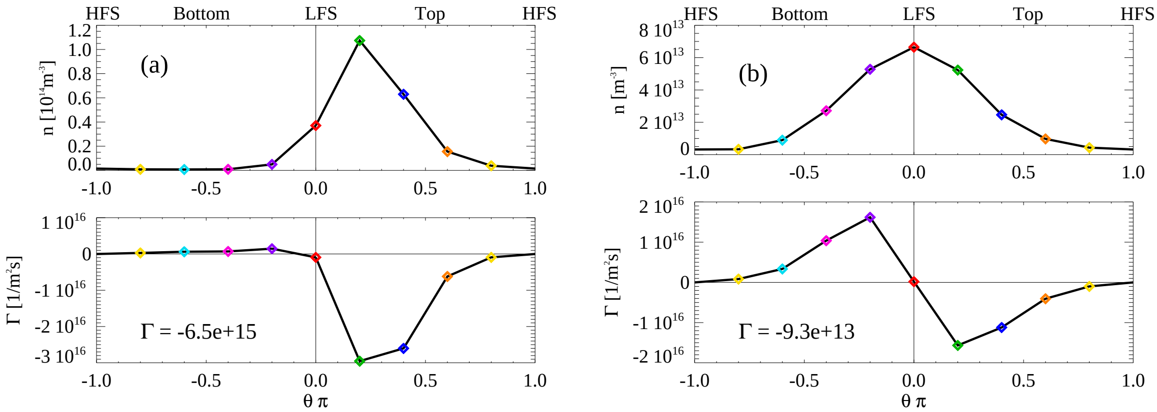

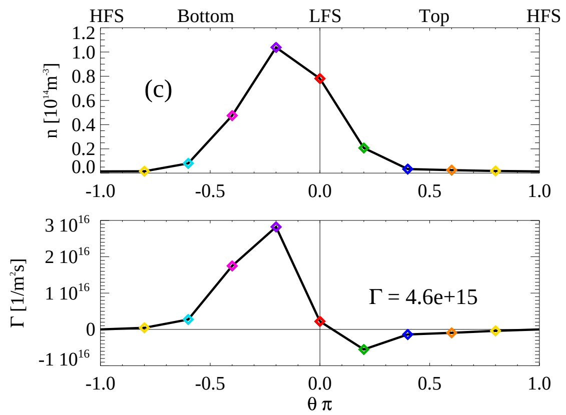

Fig. 6: Poloidal distributions of the W impurity density (top) and of the radial guiding centre W flux (bottom) for three positions of a localised W density. Values of surface averaged fluxes are also given. Results (a) and (b) are from the transient phase of a simulation, the flux is enhanced by a factor ≈ 50.

early transient phase of a simulation, where the localised density oscillates up and down, and the surface averaged W flux varies by two orders of magnitude. The steady state flux is much smaller and the W density is centered close to the midplane. These results imply that a narrow localised impurity density is normally centered near the midplane.

[1] C. Angioni, *et al.*, PPCF 54, 083028 (2014); T.C. Hender *et al.*, Nucl. Fusion 56, 066002 (2016)
[2] S.D. Pinches *et al.*, Comp. Phys. Comm. 111, 133 (1998)
[3] A. Bergmann, E. Poli, A. Peeters, Phys. Plasmas 16, 092507 (2009)
[4] T. Fülop, P. Helander, Phys. Plasmas 6, 3066 (1999)
[5] C. Angioni, P. Helander, PPCF 56, 124001 (2014)